dinates x,y through the equations

$$\tau = \int_{u=0}^{u=x/R_c} \left[1 + \frac{u^2}{(1+u^2)(\tan^2 2\vartheta - u^2)} \right]^{1/2} du \quad (12a)$$

$$\rho = \int_{u=0}^{u=1} \left[1 + \frac{w^2(u)}{1-w^2(u)} \left(\frac{xu}{R_c} + \frac{R_c}{xu} \right)^2 \right]^{1/2} du \quad (12b)$$

where the function $w(u)$ is

$$w(u) = u \sin\left(\frac{y}{R_c}\right) \exp\left[(u^2-1)\frac{x^2}{2R_c} \right] \quad (13)$$

Calculation of Crystallographic Coordinates from the Generalized Coordinates. Crystallographic coordinates (see Figure 1) can be obtained from the gc and the parameters b = C–C bond length and c = helix repeat (i.e., lattice c constant) as follows:

(i) evaluation of cylindrical coordinates l, ϕ, z for C2 and C3 atoms ($\phi_2 = 0$, $z_2 = 0$ by definition),

$$q_1 = \cos g_2 - \cos(\tfrac{2}{3}\pi - g_2) \quad (14a)$$

$$q_2 = \left(b^2 - \frac{c^2}{36} \right) \frac{c^2}{9{g_1}^2 q_1} \quad (14b)$$

$$q_3 = \frac{c^2}{18{g_1}^2 q_1}(1 + {g_1}^2 - 2g_1 \cos g_2 + g_1 q_1) \quad (14c)$$

$$l_2 = [(q_2 + {q_3}^2)^{1/2} - q_3]^{1/2} \qquad l_3 = l_2 g_1 \quad (14d)$$

$$\phi_2 = 0 \qquad \phi_3 = -g_2 \quad (14e)$$

$$z_2 = 0 \qquad z_3 = \frac{c}{6} + \frac{3 l_2 l_3 q_1}{c} \quad (14f)$$

(ii) definition of the positions of other carbon atoms of the chain C5, C6, C8, and C9 by applying the 3_1 screw operator twice; (iii) definition of the positions of the methyl side groups C1 by intersection of the cone of axis C9′–C2 and aperture $\pi - g_4$ with the cone of axis C3–C2 and aperture $\pi - g_3$ (the choice between the two possible solutions is a matter of chirality), a similar construction applies to C4 and C7 atoms; (iv) change of the origin making $z_1 = 0$ and $\phi_1 = 0$; (v) rotation of Φ of the whole helix and translation of x_0, y_0, z_0.

In the evaluation of I_{calcd} hydrogen atoms were also considered by placing them according the ideal sp^3 geometry for carbon atoms and staggered conformations for methyl groups.

Registry No. IPP, 25085-53-4.

References and Notes

(1) Immirzi, A.; Iannelli, P. *Gazz. Chim. Ital.* **1987**, *117*, 201.
(2) Rietveld, H. M. *Acta Crystallogr.* **1967**, *22*, 151.
(3) Rietveld, H. M. *J. Appl. Crystallogr.* **1969**, *2*, 65.
(4) Natta, G.; Corradini, P. *Nuovo Cimento* **1960**, Suppl. 15, 40.
(5) Mencick, Z. J. *Macromol. Sci. Phys.* **1972**, *6*, 101.
(6) Immirzi, A. *Acta Crystallogr., Sect. A* **1978**, *A34*, S348.
(7) Immirzi, A. *Acta Crystallogr., Sect. B* **1980**, *B36*, 2378.
(8) Immirzi, A. *Gazz. Chim. Ital.* **1980**, *110*, 381.
(9) Immirzi, A.; Porzio, W. *Acta Crystallogr., Sect. B* **1982**, *B38*, 2788.
(10) Hellner, E. Z. *Kristallografiya* **1954**, *106*, 122.
(11) Fraser, R. D. B.; Macrae, T. P.; Miller, A.; Rowlands, R. J. *J. Appl. Crystallogr.* **1976**, *9*, 81.
(12) Ortega, J. M.; Reinholdt, W. C. *Iterative Solution of Nonlinear Equations in Several Variables*; Academic: New York, 1970.
(13) Iannelli, P.; Immirzi, A. *Acta Crystallogr., Sect. A* **1987**, *A43*, C-199. (A full paper was submitted to Macromolecules.)
(14) Leroy, B.; Alexander, E.; Michalik, E. R. *Acta Crystallogr.* **1959**, *12*, 105.
(15) Hikosaka, M.; Seto, T. *Polym. J.* **1973**, *5*, 111.
(16) Corradini, P.; Giunchi, S.; Petraccone, V.; Pirozzi, B.; Vidal, H. M. *Gazz. Chim. Ital.* **1980**, *110*, 413.
(17) Corradini, P.; Petraccone, V.; Pirozzi, B. *Eur. Polym. J.* **1983**, *19*, 299.
(18) Corradini, P. In *Stereochemistry of Macromolecules*; Kettley, K., Eds.; M. Dekker: New York, 1968; Vol III, p 1.
(19) Benedetti, E.; Pedone, C.; Allegra, G. *Macromolecules* **1970**, *3*, 16.
(20) Bocelli, G.; Grenier-Loustalot, M. F. *Acta Crystallogr. Sect. C* **1983**, *C39*, 636.
(21) Albinati, A.; Willis, B. T. M. *J. Appl. Crystallogr.* **1982**, *15*, 361.
(22) Bürger, M. J. *X-ray Crystallography*; Wiley: New York, 1965.

Excluded-Volume Effects in Rubber Elasticity. 3. Segment Orientation[1]

J. Gao and J. H. Weiner*

Department of Physics and Division of Engineering, Brown University, Providence, Rhode Island 02912.

Received August 3, 1987; Revised Manuscript Received September 8, 1987

ABSTRACT: The effect of excluded volume on segment orientation in rubber elasticity is studied by molecular dynamics simulation of model systems of freely jointed chains with a truncated Lennard-Jones repulsive potential acting between all atoms. In a single chain with fixed end-to-end distance L and periodic boundary conditions, it is found that excluded volume causes negative orientation ($\langle P_2 \rangle < 0$) for sufficiently small L. This effect has been observed previously for a tie molecule and suggests an analogy between the confining effect of the crystalline lamellae on the tie molecule and that of excluded volume on the chain with periodic boundary conditions. In a system of three chains, corresponding to the three-chain model of rubber elasticity, it is found that intrachain excluded-volume interactions alone cause a decrease in orientation in the tensile region, but inter- and intrachain interactions together cause an increase in orientation beyond the ideal chain case. It is also found that excluded volume has a much greater effect upon the chains with end-to-end vector perpendicular to the elongation direction than upon the chain parallel to that direction.

Introduction

A rubberlike solid represents, from the atomistic viewpoint, a rather complex system. The topological character of the covalent bonds which form the long-chain molecules permits large-amplitude thermal motion of their atoms, as in a liquid, while cross-linking of these molecules supports the types of deformation characteristic of a solid. There are, in addition, noncovalent interactions between

0024-9297/88/2221-0773$01.50/0

the atoms; of these, we are here most concerned with the strongly repulsive, excluded-volume interactions which prevent any two atoms of the system from occupying the same place in space.

The classical molecular theory of rubber elasticity, which had its beginnings over 50 years ago, surmounts these complexities by focusing on the entropic character of the constituent long-chain molecules. Furthermore, the assumption based on experimental observation that the deformations of interest, e.g., uniaxial elongation, take place at constant volume means that the pressure or mean stress is determined by boundary conditions and not by the constitutive relation. The latter, therefore, need only deal with the deviatoric stress, i.e., the difference between the full stress tensor and the mean stress. If the further assumption is made that excluded-volume interactions contribute only to the mean stress, then it might appear that these interactions need not be considered explicitly in the molecular theory for the deviatoric stress.

Nevertheless, excluded volume may have significant indirect effects and in this series of papers we are exploring this possibility by means of the molecular dynamics simulation of idealized models of such systems. In the first of these papers[2] we developed the virial stress formulation for rubber elasticity. This provides a local view of stress, as opposed to the customary one which may be termed the chain view, and permits a rigorous and convenient method for the evaluation of the state of stress in the system being studied by molecular dynamics. The virial stress formulation was then applied in the second paper[3] of this series to the study of a three-chain model of rubber elasticity in uniaxial deformation. The purpose of this study was to examine the usual assumption by which the chains are regarded as ideal and noninteracting, with excluded-volume effects completely neglected. For the model studied, signififfcant indirect excluded-volume effects on the deviatoric stress were found. Furthermore, it was shown in that paper[3] how this nonideal behavior in the three-chain model of a network could be reconciled with the Flory theorem[4] which states that the behavior of a chain in a melt approaches that of an ideal chain as the melt density is increased.

An important and much studied[5] characteristic of the deformation of rubberlike materials is the development of preferred segment orientation with elongation, and in recent years various spectroscopic techniques have been developed to study this process.[6] In this paper we examine excluded volume effects on orientation by the molecular dynamics simulation of the models previously introduced. We begin, in section 1, with an examination of a single chain and continue, in section 2, with excluded volume effects on orientation in the three-chain model of rubber elasticity. In section 3, the relationship between deviatoric stress and orientation is examined and conclusions are presented in section 4.

1. Orientation in Single Chains

As before, we study a model equivalent to a freely jointed chain with a hard-sphere interaction. For computational and conceptual convenience, the covalent potential is represented by a stiff linear spring and the hard-sphere potential is replaced by a truncated Lennard-Jones potential. That is, the covalent potential $u_c(r)$ is

$$u_c(r) = \tfrac{1}{2}\kappa(r - a)^2 \tag{1.1}$$

where r is the distance between adjacent atoms on a given chain, and the noncovalent potential is

$$u_{nc}(r) = 4\epsilon\left[\left(\frac{\sigma}{r}\right)^{12} - \left(\frac{\sigma}{r}\right)^{6}\right] \quad \text{for } r \leq r_0$$
$$= u_{nc}(r_0) \quad \text{for } r \geq r_0 \tag{1.2}$$

where r denotes the distance between any nonadjacent pair of atoms and $r_0 = 2^{1/6}\sigma$. The results reported in this paper were carried out for $\kappa a^2/kT = 202.4$ and $\epsilon/kT = 0.05$. All calculations with nonzero σ employed the value $\sigma/a = 0.8$.

The atoms of the chain have positions $\mathbf{x}_k$, $k = 0, ..., N$ with $\mathbf{x}_N = L\mathbf{e}_1$. In order to avoid end effects in the noncovalent interactions, all atoms in the chain are also assumed to interact with image atoms at positions $\mathbf{x}_k + mL\mathbf{e}_1$, $k = 1, ..., N - 1$, $m = \pm1, \pm2, ...$

An outline of the molecular dynamics procedure employed is contained in the Appendix of ref 3. At each time step of the calculation and for each bond the program includes a computation of $\cos\theta$, where θ is the angle between the bond and the axial direction $\mathbf{e}_1$. A sorting routine on these computed values of $\cos\theta$ then yields the equilibrium distribution function $g(\cos\theta)$ for different values of the extension L/Na. Typical results are shown in Figure 1. One qualitative effect of excluded volume is immediately apparent. If excluded volume is neglected ($\sigma = 0$), the distribution function $g(\cos\theta)$ is concave upward for all values of L/Na whereas with excluded volume ($\sigma = 0.8a$) g becomes concave downward at sufficiently small values of L/Na.

The usual method of characterizing the distribution function $g(\cos\theta)$ is through its expansion in a series of Legendre polynomials, $P_n(\cos\theta)$. The most significant expression coefficient is $\langle P_2(\cos\theta)\rangle = \langle P_2\rangle$ where

$$\langle P_2\rangle = \tfrac{1}{2}\,(3\langle\cos^2\theta\rangle - 1) \tag{1.3}$$

and where carats denote an ensemble average, in this case an average over all bonds and time. A computation of $\langle P_2\rangle$ is included in the molecular dynamics program and typical results are shown in Figure 2 for both the ideal chain ($\sigma = 0$) and for the chain with excluded volume ($\sigma = 0.8a$). In the former case, the molecular dynamic results are compared with the theoretical expression[7]

$$\langle P_2\rangle = 1 - 3\left(\frac{L}{Na}\right)\Big/\mathcal{L}^*\left(\frac{L}{Na}\right) \tag{1.4}$$

where $\mathcal{L}^*(x)$ is the inverse Langevin function. The agreement between the molecular dynamics results for $\sigma = 0$ with eq 1.4 is seen to be quite good.

Turning next to the effect of excluded volume ($\sigma = 0.8a$), it is seen that since the dominant nonconstant term in the series expansion of $g(\cos\theta)$ is that involving P_2, the change in sign of curvature of $g(\cos\theta)$ with L/Na indicates a similar change in sign of $\langle P_2\rangle$. The variation of $\langle P_2\rangle$ with L/Na as determined by molecular dynamics for $\sigma = 0.8a$ is shown in Figure 2, and it is seen that it does become negative for small values of this parameter.

Negative values for $\langle P_2\rangle$ for small values of L/Na were also found by Petraccone et al.[8] in a model for a tie molecule confined between two crystalline lamellae, Figure 3a. In their calculations, performed on a lattice, excluded-volume effects for the atoms in the tie molecule were not included, but the bounding lamellae favored segment orientation perpendicular to the chain axis and this led to negative values of $\langle P_2\rangle$ for small L/Na. In our model, excluded-volume effects together with periodic boundary conditions apparently produce a confining effect which is similar (Figure 3c) to that of the lamellae in the calculations of Petraccone et al.[8] This analogy between the two problems is in accord with the discussion of Weiner and Stevens.[9]

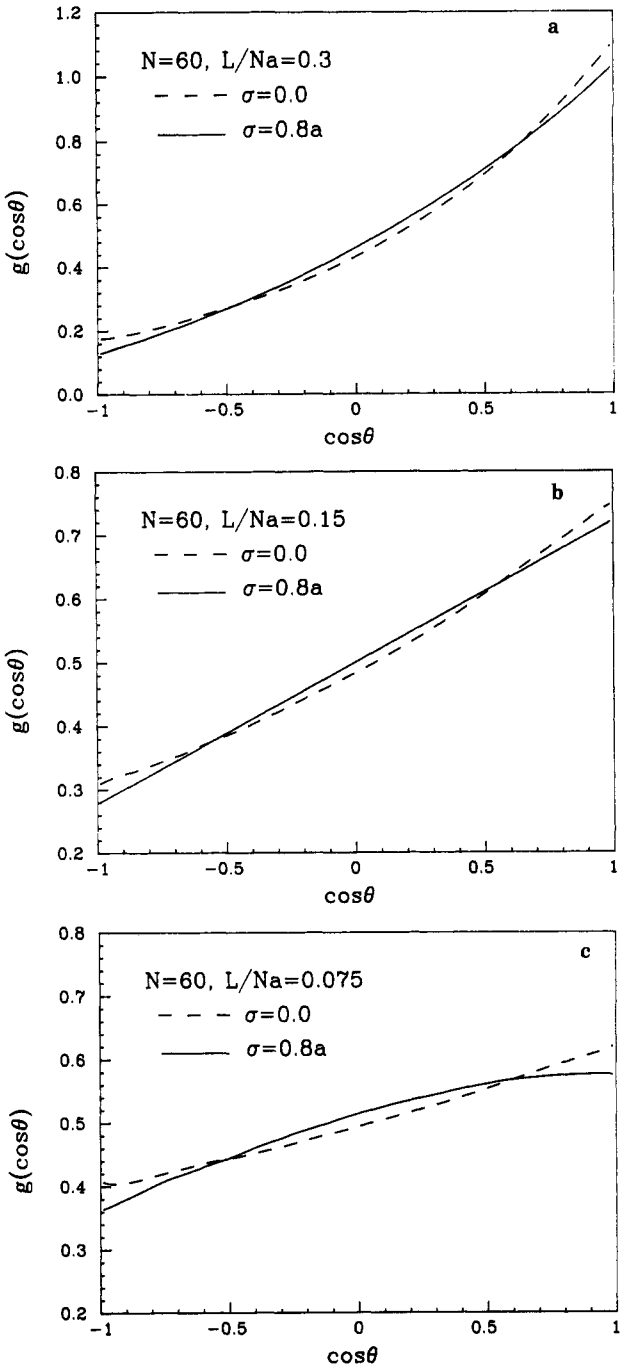

Figure 1. Distribution function g(cos θ) for a single freely jointed chain with periodic extension, where θ is the angle between the bond and the end-to-end chain vector. L is the end-to-end distance, N is number of bonds each of length a, and the parameter σ, eq 1.2, is a measure of excluded-volume diameter. (a) L/Na = 0.3; (b) L/Na = 0.15; (c) L/Na = 0.075.

The effect of excluded volume on segment orientation as measured by $\langle P_2 \rangle$ is also analogous to its effect on the time-averaged axial force $\langle f \rangle$ required to maintain a fixed end-to-end length L. In the ideal chain, $\langle f \rangle > 0$ for all values of L. However, with the consideration of excluded volume, it is found that there is a value L_0 such that $\langle f \rangle < 0$ for $L < L_0$ and the graph of the $\langle f \rangle(L)$ relation is very similar in appearance[10] to that of the $\langle P_2 \rangle(L)$ relation. This similarity is more than fortuitous and we return to this question in section 3 in terms of the relation between stress and orientation.

2. Three-Chain Model

We consider next a system which models a cross-linked network of the freely jointed, hard-sphere chains. The

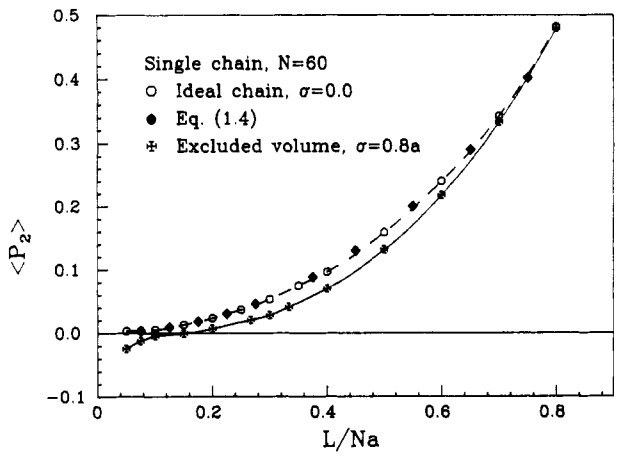

Figure 2. Orientation function, $\langle P_2 \rangle = \langle P_2(\cos\theta) \rangle$, for a single freely jointed chain with periodic extension, where θ is the angle between the bond and the end-to-end chain vector, as determined for an ideal chain (σ = 0) by molecular dynamics and by theory (eq 1.4) and for chain with excluded volume (σ = 0.8a) by molecular dynamics.

system is based on the familar three-chain model of rubber elasticity.[11] To construct the system in the reference state, we start with a cube of side L_0 centered at the origin of a rectangular cartesian coordinate system. Three chains, each with N bonds, are located in the cube with one chain running in each coordinate direction with its end atoms fixed in the center of the cube planes perpendicular to that direction. Periodic boundary conditions are employed in all three coordinate directions. The system is subjected to a uniaxial deformation at constant volume so that the cube side in the x_1 direction has length λL_0, while the other two sides have length $\lambda^{-1/2} L_0$.

Molecular dynamics simulation of this model is carried out as described in the Appendix to ref 3. This program also computes $\langle P_2(\cos\theta) \rangle$ where, in contrast to the discussion of the single chain in section 1, here θ is the angle between any bond of the system and the direction of elongation, x_1.

For an ideal Gaussian network, theory predicts

$$\langle P_2 \rangle = \frac{1}{5N}(\lambda^2 - \lambda^{-1}) \tag{2.1}$$

The numerical results for no excluded volume (σ = 0) are shown in Figure 4 where they are compared with the theoretical prediction of eq 2.1. The agreement is seen to be quite good; the slight discrepancy at the larger values of λ may be attributed to the non-Gaussian behavior of the finite chains of the model.

We turn next to calculations for the three-chain model with excluded volume, σ = 0.8a, and distinguish between (a) the case of noninteracting chains, i.e., intrachain excluded volume effects only, and (b) interacting chains, i.e., inter- and intrachain excluded-volume effects. Calculations were performed for a reduced system density ρ = 0.18, where ρ is defined as

$$\rho = 3(N + 1)\sigma^3/L_0^3 \tag{2.2}$$

The results are shown in Figure 5, where they are compared to the case of noninteracting ideal chains, σ = 0. It is seen that intrachain excluded-volume effects by themselves decrease $\langle P_2 \rangle$ in the tensile region. However, both inter- and intrachain excluded volume effects together produce a substantial increase.

It is of interest to examine the simulation results in greater detail to understand how these changes in orientation are effected. The results shown in Figure 5 showed

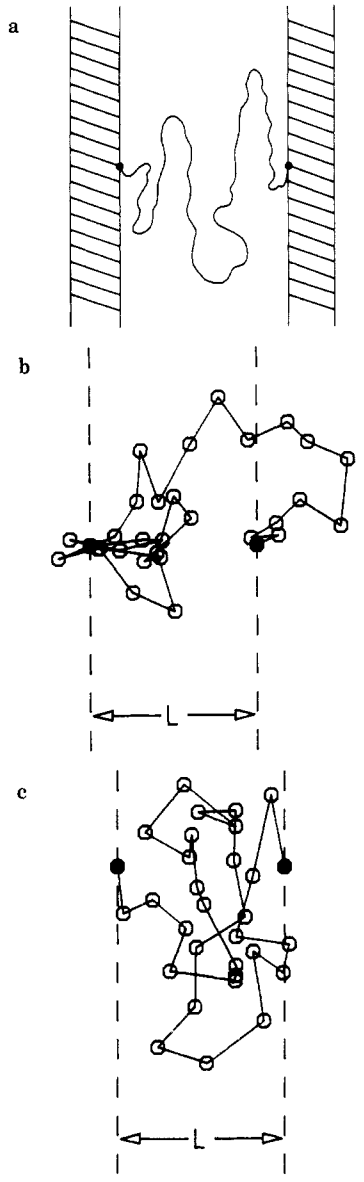

Figure 3. Analogy between the confinement effect of crystalline lamellae on the tie molecule and of excluded volume on atoms of a periodically extended single chain. (a) Schematic of tie molecule between crystalline lamellae as discussed by Petraccone et al.[8] (b) Instantaneous positions of atoms and bonds as obtained from molecular dynamics simulation and projected onto a plane containing an end-to-end vector of length L. Atoms shown in black are fixed. No excluded volume, $\sigma = 0$. (c) Same as (b) but with excluded volume, $\sigma = 0.8a$. Note that excluded-volume interactions with atoms of periodic extension of chain confine atoms of principal chain to a strip of width L and favor a bond orientation perpendicular to the end-to-end chain vector.

the value of $\langle P_2 \rangle$ as determined by averaging over all of the bonds of the system, without regard to the chain to which a particular bond belongs. For the uniaxial deformation in the x_1 direction under study here, we now consider a decomposition of $\langle P_2 \rangle$ of the form

$$\langle P_2 \rangle = \tfrac{1}{3}\langle P_2 \rangle_{\parallel} + \tfrac{2}{3}\langle P_2 \rangle_{\perp} \qquad (2.3)$$

where $\langle P_2 \rangle_{\parallel}$ is the average over all bonds in the chain whose end-to-end vector lies in the x_1 direction, termed the longitudinal chain, while $\langle P_2 \rangle_{\perp}$ is the average over each of the chains with end-to-end vectors in the x_2 and x_3 directions, the transverse chains. In all cases, θ, the bond orientation, is measured from the x_1 direction. In this connection we note that, for rotationally symmetric chains, if ϕ is measured from the end-to-end chain vector $\mathbf{r}$ and

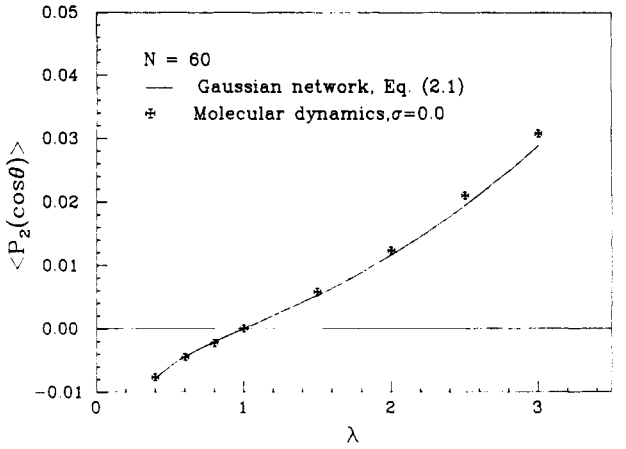

Figure 4. Comparison of the molecular dynamics simulation of a three-chain model with no excluded volume ($\sigma = 0$) with theoretical prediction for Gaussian network, eq. 2.1. θ is angle between any bond of system and extension direction, x_1.

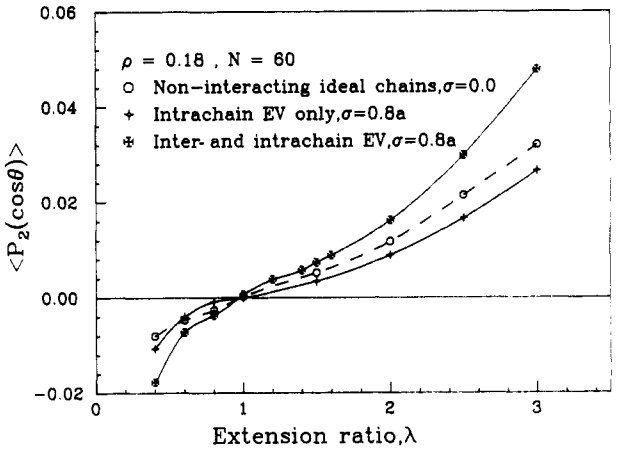

Figure 5. Effect of excluded volume (EV) on bond orientation in a three-chain model; θ is the angle between any bond of system and extension direction, x_1. Reduced system density ρ defined in eq 2.2.

θ is measured from a direction perpendicular to $\mathbf{r}$, then it follows from simple geometric considerations that

$$\langle P_2(\cos\theta) \rangle = -\tfrac{1}{2}\langle P_2(\cos\phi) \rangle \qquad (2.4)$$

The results of this decomposition are shown in Figure 6. Three curves are presented for both $\langle P_2 \rangle_{\parallel}$ and $\langle P_2 \rangle_{\perp}$: (i) ideal chains, $\sigma = 0$; (ii) chains with $\sigma = 0.8$, no interchain interaction; and (iii) chains with $\sigma = 0.8$, inter- and intrachain interaction. The first two curves are obtained from the single-chain results shown in Figure 2, but are plotted against λ instead of against L/Na. (Recall that $L = \lambda L_0$ for longitudinal chains, while $L = \lambda^{-1/2} L_0$ for transverse chains.) Also, in the case of transverse chains, eq 2.4 is employed since, in Figure 6, θ is measured from the x_1 direction for the transverse chains as well as for the longitudinal chain. It is seen that interchain interaction causes an increase in orientation in the tensile region for both longitudinal and transverse chains. However, this increase is modest for longitudinal chains and leaves $\langle P_2 \rangle_{\parallel}$ substantially below that for the ideal chain, whereas the increase due to interchain interaction is quite large for $\langle P_2 \rangle_{\perp}$. It is the latter effect which is responsible for the overall increase in $\langle P_2 \rangle$ observed in Figure 5 when both inter- and intrachain excluded-volume effects are considered.

3. Stress-Orientation Relation

An important question is the relationship between the stress imposed on a rubberlike solid and the segment or

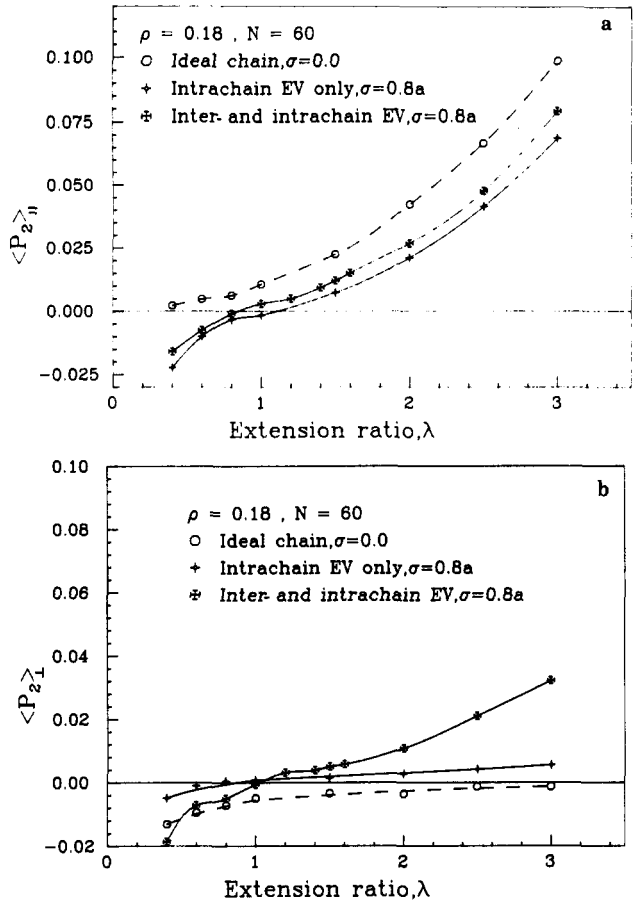

Figure 6. Effect of excluded volume on bond orientation of (a) longitudinal chains, $\langle P_2 \rangle_{\parallel}$, and of (b) transverse chains, $\langle P_2 \rangle_{\perp}$.

bond orientatioin produced by the resulting deformation. The usual theoretical treatments of this question, based on the chain view of stress, takes place in two stages: (a) The imposed macroscopic deformation produces a corresponding change in distribution in the end-to-end chain vectors of the system. This change is expressed most simply in terms of the affine assumption or by means of more advanced theories, such as the constrained-junction theory of Flory and Erman.[12,13] (b) The change in bond orientation is then deduced from the change in end-to-end vector distribution.

For the case of the present freely jointed model in uniaxial deformation, the virial stress formula, discussed in ref 2 and used in ref 3, provides a more direct and transparent relationship between stress and orientation. In those references, the components of the full stress tensor referred to a rectangular cartesian coordinate system x_i, $i = 1, 2, 3$, are denoted by t_{ij}. As noted there, in a system treated as incompressible, only the deviatoric stress $\tau_{ij} = t_{ij} - {}^1/_3\,\delta_{ij}t_{kk}$ is determined by the constitutive relation. Here δ_{ij} is the Kronecker delta and ${}^1/_3 t_{kk}$ (summation on repeated indices) is the mean stress to be determined from the boundary conditions. For the case of uniaxial deformation in the x_1 direction, $t_{22} = t_{33}$ and $\tau_{11} = {}^2/_3(t_{11} - t_{22})$. Furthermore, the computer simulation results of ref 3 showed that the noncovalent hard-sphere potential made almost a purely isotropic contribution to the stress tensor t_{ij} or, equivalently, the deviatoric stress was due almost entirely to the covalent interactions. Under these conditions, the virial formula for the deviatoric stress component τ_{11} is (see eq 2.5 of ref 3)

$$\tau_{11} = \frac{1}{3v}\sum_{\alpha\in c}\langle r_\alpha u_c'(r_\alpha)[3\cos^2\theta_\alpha - 1]\rangle \qquad (3.1)$$

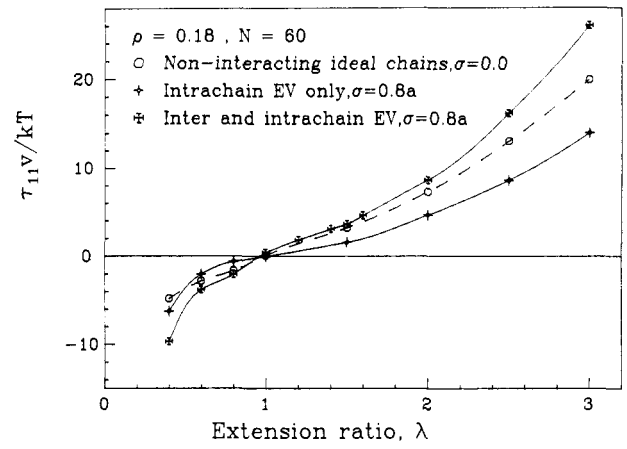

Figure 7. Deviatoric stress, τ_{11}, in a three-chain model.

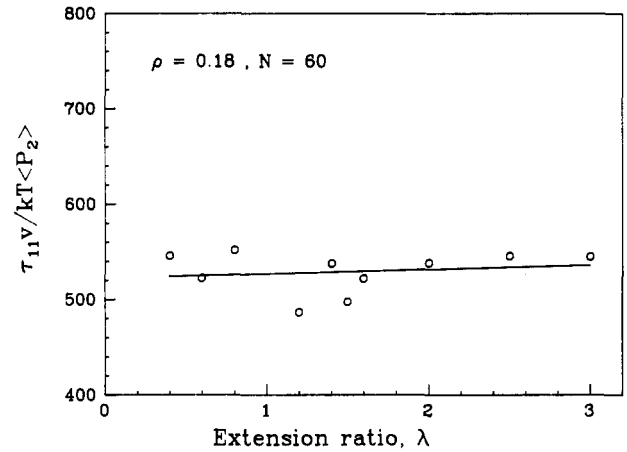

Figure 8. Ratio of deviatoric stress, τ_{11}, to orientation function, $\langle P_2 \rangle$. Curve shown is a straight line corresponding to a least-square fit to computed points.

where $u_c(r)$ is the covalent potential defined in eq 1.1, u_c' is its derivative, the sum is over all of the bonds in the volume $v = L_0{}^3$, and θ_α is the angle between the α bond and the x_1 axis. In the present notation, eq 3.1 can be rewritten as

$$\tau_{11} = \frac{2}{3v}\sum_{\alpha\in c}\langle r_\alpha u_c'(r_\alpha)P_2(\cos\theta_\alpha)\rangle \qquad (3.2)$$

a form which makes the relation between stress and orientation quite transparent.

The variation in deviatoric stress τ_{11} with λ for the three-chain model as computed from the molecular dynamics simulation by means of the virial stress formula is shown in Figure 7. The strong similarity between the nature of stress variation shown in this figure and the overall orientation variation shown in Figure 5 is apparent. The ratio of $\tau_{11}/\langle P_2 \rangle$ is shown in Figure 8 and is seen to be reasonably constant.

Conclusions

The computer studies of the hard-sphere, freely jointed system reveal significant excluded-volume effects upon bond orientation. Particular observations are as follows:

(1) In a single chain with fixed end-to-end distance L, which interacts through periodic boundary conditions with an infinitely extended chain, excluded-volume effects are found to produce negative orientation, $\langle P_2 \rangle < 0$, for sufficiently small L/Na. This result is similar to that found earlier by Petraccone et al.[8] in a model without excluded volume for a tie molecule confined between two crystalline lamellae and serves to demonstrate the analogy between

the two problems discussed earlier by Weiner and Stevens.[9]

(2) In the three-chain model it is found that intrachain excluded-volume interactions alone cause a decrease in orientation in the tensile region, as compared to the ideal chain case, but a substantial increase in orientation as compared to the ideal chain case occurs if interchain interactions are included as well.

(3) It might be expected that the effect of excluded volume on bond orientation in an amorphous network should be independent of the end-to-end vector of the chain to which the bond belongs. This is the assumption made by Tanaka and Allen[14] in their refinement of the DiMarzio analysis[15] of the packing effect in rubber elasticity. The present computer studies of the uniaxial deformation of the three-chain model, however, show that bonds in the longitudinal chain (end-to-end vector in the direction of deformation) and those in the transverse chains (end-to-end vector perpendicular to the direction of deformation) are affected differently by excluded volume. Referring always to the tensile regime, it is found that intrachain interactions alone cause a large decrease in orientation, i.e., in $\langle P_2 \rangle$, for longitudinal chains but these interactions cause an increase and change in sign in orientation for transverse chains. If interchain interactions are included as well, then there is an increase in $\langle P_2 \rangle$ for both longitudinal and transverse chains. However, the former increase is modest, leaving the value of $\langle P_2 \rangle_\parallel$ still below that of the ideal chain, whereas the increase in $\langle P_2 \rangle_\perp$ is large. It is the latter effect that is responsible for the overall increase in $\langle P_2 \rangle$ in the tensile region.

(4) The virial stress formulation for the deviatoric stress component τ_{11} for uniaxial deformation in the x_1 direction exhibits the dependence of τ_{11} upon bond orientation in a more direct manner than does the usual chain view of stress.

Molecular dynamics simulations of the three-chain model yield a ratio of $\tau_{11}/\langle P_2 \rangle$ which is reasonably constant ($\pm 5\%$) over an extension range $0.4 < \lambda < 3$. This is in contrast to the recent results of Erman and Monnerie[5] who conclude on the basis of the constrained-junction theory of Flory and Erman[11,12] that orientation is not proportional to stress in real networks. The effect of junction fluctuation is, of course, absent from the three-chain model.

(5) The large excluded-volume effects on bond orientation in the present three-chain model of rubber elasticity are in contrast to the relatively weak excluded-volume effect on the molecular optical anisotropy of polymers found by Lemaire et al.[16] by Monte Carlo calculations for chains constrained to a tetrahedral lattice and by Mattice and Saiz[17] for realistic rotational isomeric state models for six types of polymers, although appreciable effects in racemic vinyl polymers were found in the latter study. In both of these works, isolated free molecules with unconstrained end-to-end vectors were studied as is appropriate for dilute polymer solutions. The present work indicates that excluded volume will have a much stronger effect on bond orientation in polymer networks in which end-to-end vectors are subject to some constraint.

(6) An assumption in some theories of rubber elasticity is that the network can be regarded as a system of noninteracting ideal chains. This assumption was examined in ref 3 on the basis of a comparison of the stress predicted by it and that determined by the virial stress formula applied to a molecular dynamics simulation. The present study of excluded-volume effects on orientation serves to cast further doubt on the validity of this assumption, which may be stated also in the form that the configurations of the polymer chains are unperturbed by their neighbors. However, the large change in bond orientations due to excluded-volume interchain interactions reflects correspondingly large changes in the chain configuration distribution and shows that this is not the case for the model studied here.

Other more recent theories of rubber elasticity introduce noncovalent interactions through their effect on cross-link fluctuations,[18-21] as confining tubes[22-27] or entangling slip-links.[28] The extent to which these approaches serve to represent the excluded-volume effects as seen in more fully atomistic treatments remains a subject for future study.

References and Notes

(1) This paper is based on the research of J. Gao performed in partial fulfillment of the requirements for the Ph.D. in Physics at Brown University. This work has been supported by the Gas Research Institute (Contract 5085-260-1152), by the National Science Foundation through the Materials Research Laboratory, Brown University, and by the National Science Foundation, Polymers Program, which provided computer time at the National Center for Supercomputing Applications, University of Illinois, and at the Pittsburgh Supercomputing Center.
(2) Gao, J.; Weiner, J. H. *Macromolecules* **1987**, *20*, 2520.
(3) Gao, J.; Weiner, J. H. *Macromolecules* **1987**, *20*, 2525.
(4) Flory, P. J. *J. Chem. Phys.* **1949**, *17*, 303. The term "Flory theorem" for this result has been suggested by: deGennes, P.-G. *Scaling Concepts in Polymer Physics*; Cornell University Press: Ithaca, NY, 1979; p 54.
(5) See, for example: Erman, B.; Monnerie, L. *Macromolecules* **1985**, *18*, 1985 and references cited therein.
(6) For a brief review, see: Mitchell, G. R.; Brown, D. J.; Windle, A. J. *Polymer* **1985**, *26*, 1755 and further references cited therein.
(7) Kuhn, W.; Grün, F. *Kolloid-Z.* **1943**, *101*, 248. See the discussion of the derivation of Kuhn and Grün in: Flory, P. J. *Statistical Mechanics of Chain Molecules*; Interscience: New York, 1969; p 369.
(8) Petraccone, V.; Sanchez, I. C.; Stein, R. S. *J. Polym. Sci., Polym. Phys. Ed.* **1975**, *13*, 1991.
(9) Weiner, J. H.; Stevens, J. W. *Macromolecules* **1983**, *16*, 672.
(10) Gao, J.; Weiner, J. H. *Macromolecules* **1987**, *20*, 142.
(11) Treloar, L. R. G. *The Physics of Rubber Elasticity*; 3rd ed.; Clarendon: Oxford, 1975; pp 113–116.
(12) Flory, P. J.; Erman, B. *Macromolecules* **1982**, *15*, 800.
(13) Erman, B.; Flory, P. J. *Macromolecules* **1982**, *15*, 806.
(14) Tanaka, T.; Allen, G. *Macromolecules* **1977**, *10*, 426.
(15) DiMarzio, E. A. *J. Chem. Phys.* **1962**, *36*, 1563.
(16) Lemaire, B.; Fourche, G.; Sanchez, E. *J. Polym. Sci., Polym. Phys. Ed.* **1974**, *12*, 417.
(17) Mattice, W. L.; Saiz, E. *J. Polym. Sci., Polym. Phys. Ed.* **1986**, *24*, 2669.
(18) Ronca, G.; Allegra, G. *J. Chem. Phys.* **1975**, *63*, 4990.
(19) Flory, P. J. *Proc. R. Soc. London, A.* **1976**, *351*, 351.
(20) Flory, P. J.; Erman, B., loc. cit.
(21) Erman, B.; Flory, P. J., loc. cit.
(22) Edwards, S. F. *Proc. Phys. Soc.* **1967**, *92*, 9.
(23) DiMarzio, E. A. *Polym. Prepr. (Am. Chem. Soc., Div. Polym. Chem.)* **1968**, *9* (1), 256.
(24) deGennes, P.-G. *J. Phys. Lett.* **1974**, *35*, L-133.
(25) Gaylord, R. J. *Polym. Eng. Sci.* **1979**, *19*, 263.
(26) Marucci, G. *Macromolecules* **1981**, *14*, 434.
(27) Gaylord, R. J.; Douglas, J. F. *Polym. Bull.*, in press.
(28) Doi, M.; Edwards, S. F. *J. Chem. Soc., Faraday Trans. 2* **1978**, *74*, 1802.